Cell Reports

Report

Histone H3 Methylated at Arginine 17 Is Essential for Reprogramming the Paternal Genome in Zygotes

Graphical Abstract

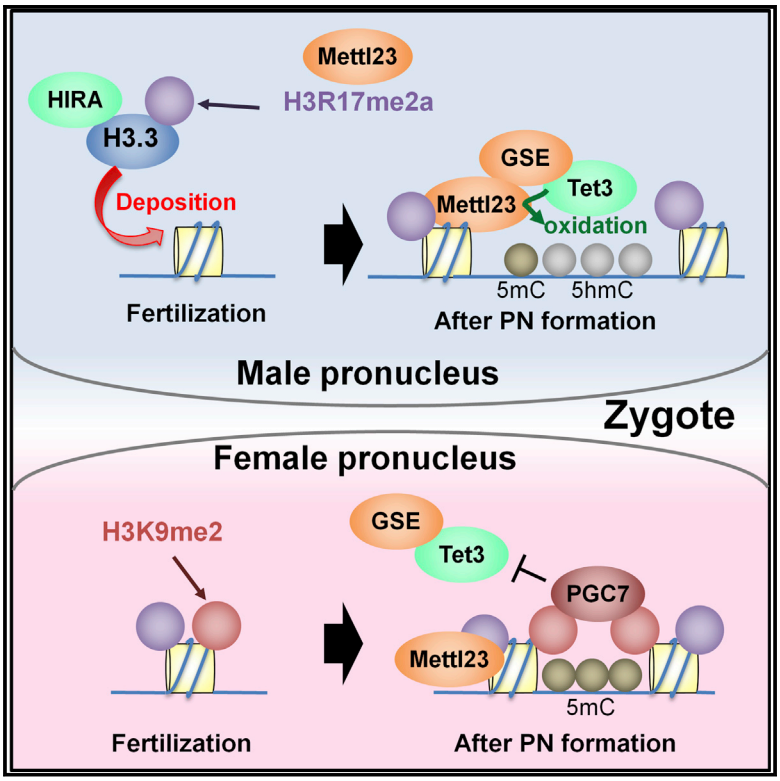

Authors

Yuki Hatanaka, Takeshi Tsusaka, Natsumi Shimizu, ..., Kazuya Matsumoto, Yoichi Shinkai, Atsuo Ogura

Correspondence

yuki.hatanaka@riken.jp (Y.H.), kazum@waka.kindai.ac.jp (K.M.), ogura@rtc.riken.go.jp (A.O.)

In Brief

Maternal factors mediate nucleosome assembly and active DNA demethylation of the paternal genome during reprogramming in mouse oocytes; however, the underlying mechanisms are poorly described. Hatanaka et al. show that maternally provided H3R17me2a is responsible not only for H3.3 incorporation but also for active DNA demethylation in the paternal genome.

Highlights

- Mettl23 is an arginine methyltransferase that catalyzes H3R17me2a in mouse oocytes
- H3R17me2a is responsible for H3.3 incorporation and active DNA demethylation
- Mettl23 interacts with Tet3 via gonad-specific expression (GSE) protein
- GSE and Mettl23 are indispensable for active DNA demethylation

Hatanaka et al., 2017, Cell Reports *20*, 2756–2765
September 19, 2017 © 2017 The Author(s).
http://dx.doi.org/10.1016/j.celrep.2017.08.088

CellPress

OPEN ACCESS
CellPress

Cell Reports
Report

Histone H3 Methylated at Arginine 17 Is Essential for Reprogramming the Paternal Genome in Zygotes

Yuki Hatanaka,[1,*] Takeshi Tsusaka,[2,3] Natsumi Shimizu,[4] Kohtaro Morita,[4] Takehiro Suzuki,[5] Shinichi Machida,[6] Manabu Satoh,[4] Arata Honda,[1,7] Michiko Hirose,[1] Satoshi Kamimura,[1,8] Narumi Ogonuki,[1] Toshinobu Nakamura,[9] Kimiko Inoue,[1,8] Yoshihiko Hosoi,[4] Naoshi Dohmae,[5] Toru Nakano,[10] Hitoshi Kurumizaka,[6] Kazuya Matsumoto,[4,*] Yoichi Shinkai,[2] and Atsuo Ogura[1,8,11,12,*]

[1]RIKEN BioResource Center, Ibaraki 305-0074, Japan
[2]Cellular Memory Laboratory, RIKEN Wako, Saitama 351-0198, Japan
[3]Department of Diabetes, Endocrinology and Nutrition, Graduate School of Medicine, Kyoto University, Kyoto 606-8507, Japan
[4]Division of Biological Science, Graduate School of Biology-Oriented Science and Technology, Kindai University, Wakayama 649-6493, Japan
[5]RIKEN Center for Sustainable Resource Science, Wako, Saitama 351-0198, Japan
[6]Laboratory of Structural Biology, Graduate School of Advanced Science and Engineering, Waseda University, 2-2 Wakamatsu-cho, Shinjuku-ku, Tokyo 162-8480, Japan
[7]Organization for Promotion of Tenure Track, University of Miyazaki, Miyazaki 889-1692, Japan
[8]Graduate School of Life and Environmental Sciences, University of Tsukuba, Ibaraki 305-8572, Japan
[9]Department of Bio-Science, Nagahama Institute of Bio-Science and Technology, Shiga 526-0829, Japan
[10]Department of Pathology, Graduate School of Medicine, Osaka University, Osaka 565-0871, Japan
[11]Center for Disease Biology and Integrative Medicine, Faculty of Medicine, University of Tokyo, Tokyo 113-0033, Japan
[12]Lead Contact
*Correspondence: yuki.hatanaka@riken.jp (Y.H.), kazum@waka.kindai.ac.jp (K.M.), ogura@rtc.riken.go.jp (A.O.)
http://dx.doi.org/10.1016/j.celrep.2017.08.088

SUMMARY

At fertilization, the paternal genome undergoes extensive reprogramming through protamine-histone exchange and active DNA demethylation, but only a few maternal factors have been defined in these processes. We identified maternal Mettl23 as a protein arginine methyltransferase (PRMT), which most likely catalyzes the asymmetric dimethylation of histone H3R17 (H3R17me2a), as indicated by in vitro assays and treatment with TBBD, an H3R17 PRMT inhibitor. Maternal histone H3.3, which is essential for paternal nucleosomal assembly, is unable to be incorporated into the male pronucleus when it lacks R17me2a. Mettl23 interacts with Tet3, a 5mC-oxidizing enzyme responsible for active DNA demethylation, by binding to another maternal factor, GSE (gonad-specific expression). Depletion of Mettl23 from oocytes resulted in impaired accumulation of GSE, Tet3, and 5hmC in the male pronucleus, suggesting that Mettl23 may recruit GSE-Tet3 to chromatin. Our findings establish H3R17me2a and its catalyzing enzyme Mettl23 as key regulators of paternal genome reprogramming.

INTRODUCTION

Mammalian development is regulated by the precise orchestration of a series of epigenetic events, which are heritable changes in gene expression that do not involve changes to the underlying DNA sequence. Reprogramming of the paternal genome in mammals is essential for establishing the totipotent state of the zygotic genome at fertilization (Hackett et al., 2012; Sasaki and Matsui, 2008). This reprogramming initiates with the removal of protamine from the decondensing nucleus of the fertilizing sperm. The paternal genome then forms the male pronucleus (PN) with nucleosomes containing maternally derived core histones (Lin et al., 2014; Inoue and Zhang, 2014). At this stage, the methylation level of paternal DNA is higher than that of maternal DNA, but later, active DNA demethylation proceeds predominantly in the male PN, leading to an asymmetric epigenetic status that discriminates the parental genomes during the early cleavage stages (Inoue and Zhang, 2011). To date, several maternal factors responsible for these dynamic reprogramming processes have been identified, especially in mice.

Maternal core histones are incorporated into the nucleosomal structure in the male PN. The major histone variants involved in this process are H2A.X and H3.3 (Nashun et al., 2010; Lin et al., 2014). As H2A.X is also incorporated into the maternal genome by replacing H2A.Z, it is assumed that this H2A variant exchange is responsible for establishment of the new epigenetic memory at fertilization (Nashun et al., 2010). By contrast, H3.3 is incorporated exclusively to the male PN, because the maternal genome already possesses H3.3 before fertilization. Therefore, depletion of the maternal HIRA, the histone H3.3 chaperone, resulted in the impairment of the male, but not female, PN formation in zygotes (Inoue and Zhang, 2014; Nashun et al., 2015). This finding indicates that HIRA-mediated H3.3 deposition plays a key role in paternal genomic reprogramming.

This is an open access article under the CC BY-NC-ND license (http://creativecommons.org/licenses/by-nc-nd/4.0/).

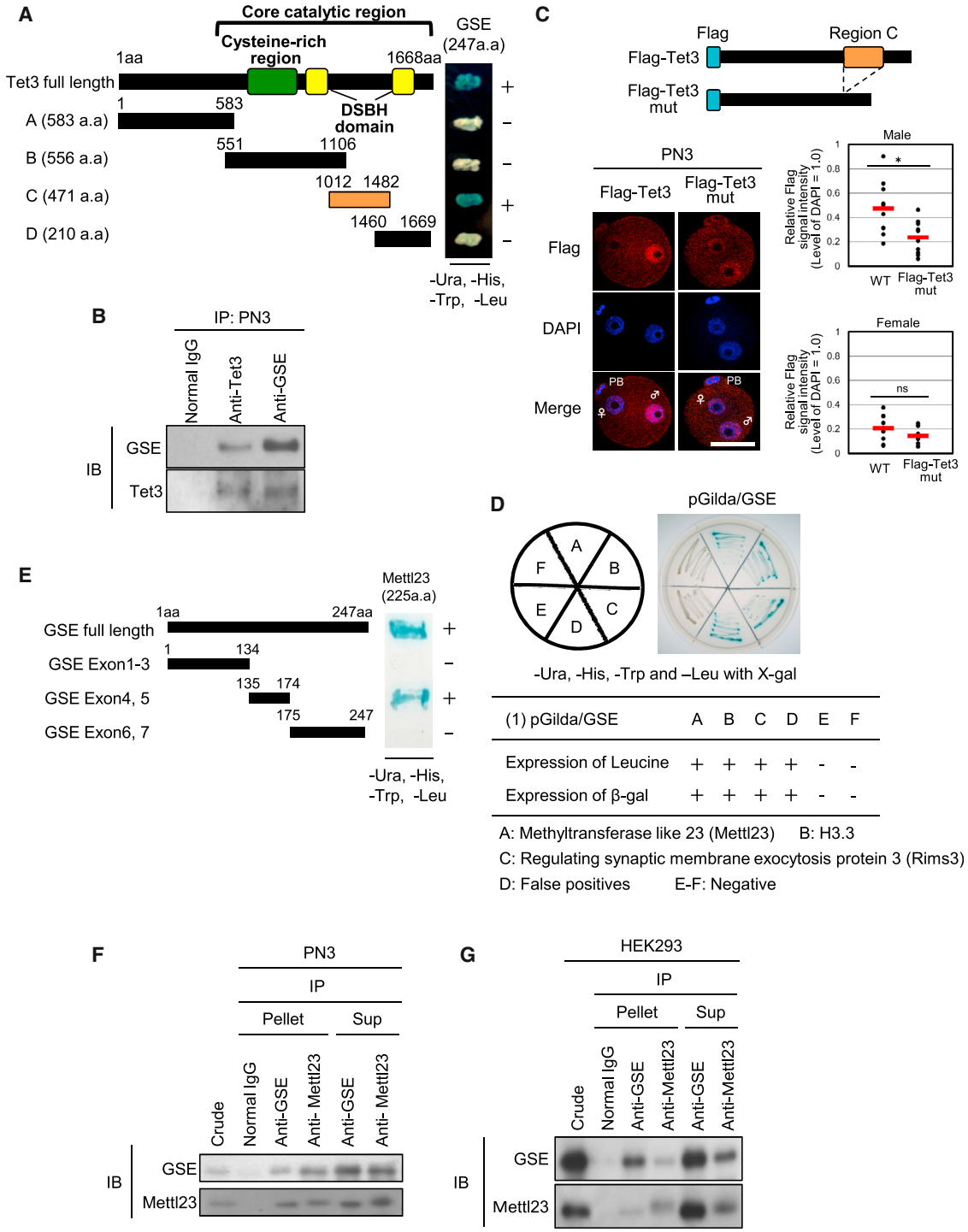

Figure 1. GSE Protein Interacts with Tet3 and Mettl23 in Mouse Zygotes

(A) Interaction of GSE with Tet3 analyzed using a yeast two-hybrid assay. The full-length and truncated Tet3 (~471 aas; region C) interacted with GSE, as indicated by the blue colonies.

(B) Interaction of GSE with Tet3 in PN3 zygotes, as demonstrated by coimmunoprecipitation using specific antibodies. A representative result from three replicate experiments each using 100–150 zygotes.IgG, immunoglobulin G.

(C) The effect of deletion of the domain C in FLAG-Tet3 on Tet3 accumulation in male pronucleus of FLAG-Tet3 mRNA-injected PN3 zygotes. Left: DNA was stained with DAPI. PB, the second polar body. Scale bar, 50 μm. Right: the relative FLAG signal intensities in the male and female PNs. The level of DAPI was set as 1.0. Red bars indicate the mean ratios. *$p < 0.01$ (versus FLAG-Tet3-injected); ns, not significant. Ten zygotes were analyzed for each group.

(legend continued on next page)

Previously, we have found that the gonadal-specific expression (GSE) protein, a maternal factor that is specifically expressed in germ cells, might be involved in active DNA demethylation during zygotic development (Hatanaka et al., 2013; Mizuno et al., 2006). Therefore, in this study, we examined whether GSE would interact with Tet3, an oxidative enzyme responsible for active DNA demethylation by conversion of 5-methylcytosine (5mC) to 5-hydroxymethylcytosine (5hmC) (Gu et al., 2011), and whether other maternal factors might exist to recruit Tet3 to its target sites. We identified methyltransferase-like 23 (Mettl23) as a Tet3-related factor. Mettl23 is an arginine methyltransferase that catalyzes asymmetric dimethylation of histone H3 at arginine 17 (H3R17me2a). Importantly, we found that R17me2a was responsible for the incorporation of maternal H3.3 into the male PN.

RESULTS

GSE Protein Interacts with Tet3 in Zygotes

As we have already identified GSE as a putative maternal factor involved in active DNA demethylation, we examined whether GSE interacted with Tet3 protein by a yeast two-hybrid system. As shown in Figure 1A, GSE interacted not only with the full-length Tet3 but also with a part of its core catalytic region that has methylcytosine dioxygenase activity from amino acids (aas) 1012–1482 (region C in Figure 1A). This region is conserved in the *Tet* family of genes (Kohli and Zhang, 2013; Pastor et al., 2013; Tan and Shi, 2012). We next performed coimmunoprecipitation experiments using anti-GSE and anti-Tet3 antibodies and confirmed that GSE interacted with Tet3 in zygotes at the pronuclear 3 (PN3) stage (Figure 1B). Furthermore, we observed that the deletion of region C in Tet3 resulted in the impairment of Tet3 recruitment into the male PN, as indicated by the decrease of the signal intensity in Figure 1C. These results suggest that the interaction of GSE and Tet3 is responsible for the recruitment of Tet3 into the male PN in zygotes.

GSE Interacts with Mettl23 in Zygotes

GSE could be associated with core histones, as indicated by a yeast two-hybrid assay (Figure S1A), but it has no functional domains that could modify histone proteins (Mizuno et al., 2006). Therefore, we hypothesized that there might be another factor intercalating between GSE and core histones to recruit Tet3-GSE to target sites. To test this, we first searched for interacting proteins in a yeast two-hybrid screening of a mouse ovary cDNA library using the GSE protein as bait and identified Mettl23, histone H3.3, and Rims3 as GSE-interacting proteins (Figure 1D). Rims3 is known to be involved in exocytosis and is expressed primarily in the nervous system. Therefore, we focused on Mettl23, a putative methyltransferase, as a candidate maternal factor interacting with the Tet3-GSE complex. We have previously shown that transcription of the GSE gene involves splicing variants: a long form of the protein (27.6 kDa) involving all exons, and a short form (23.1 kDa) with exons 4–5 not transcribed. As the long form was expressed from the zygote-to-blastocyst stages (Hatanaka et al., 2013), we tested whether Mettl23 would interact with the long form of GSE using a yeast two-hybrid system. Mettl23 interacted with the product of exons 4–5 as well as the full-length form, indicating that it was associated with the long form in zygotes (Figure 1E). In agreement with this, Mettl23 was expressed from oocytes through the preimplantation stages, in addition to several other tissues (Figures S1B and S1C). We confirmed interaction of Mettl23 with GSE in PN3 zygotes by a coimmunoprecipitation assay using pooled zygotes (Figure 1F). Their direct binding was also confirmed by an assay using His-tagged Mettl23 and His-tagged GSE proteins purified from transfected HEK293 cells (Figure 1G). These results suggested that Mettl23 is a binding partner of GSE in zygotes.

Mettl23 Is Responsible for the Accumulation of H3R17me2a into PNs during Zygotic Development

Mettl23 belongs to a methyltransferase-like (Mettl) family that has distant homology with protein arginine methyltransferases (PRMTs), but its enzymatic activity has not yet been defined (Cloutier et al., 2013). We found that Mettl23 has homology with the conserved domains of PRMT activity in PRMT1–8 (Figure 2A).

Next, we confirmed the PRMT activity of Mettl23 in metaphase II (MII) oocytes using Mettl23-knockdown (Mettl23-KD) oocytes, which had been injected with short interfering (si)RNA specific for *Mettl23*. Mettl23-KD specifically decreased the level of H3R17me2a but not the level of other arginine methylation residues in oocytes (Figure 2B; see also Figure S2A). Immunoblot analysis indicated the localization of H3R17me2a in germinal vesicle (GV)-stage and MII oocytes and preimplantation embryos until the blastocyst stage (Figure S2B). In PN3-stage zygotes, Mettl23 was localized in both PNs and cytoplasm in association with nuclear H3R17me2a (Figure S2C). We also noted that Mettl23, as well as H3R17me2a, were distributed symmetrically in both PNs (Figure S2C), as indicated by the M/F fluorescence ratio of approximately 1.0 (Figure S2D). This behavior was in contrast to that of GSE, which showed a predominant distribution in the male PN (Figure 3F).

To demonstrate the PRMT activity of Mettl23, we performed in vitro assays in the presence of recombinant histone H3.1 by using 3xFLAG-His6-Mettl23 purified from transfected HEK293T cells. As shown in Figure 2C, the Mettl23 protein methylated histone H3.1; this H3.1 methylation was reduced by treatment with TBBD (ellagic acid), which specifically inhibits methylation at H3R17 by binding to KAPR^{17}K aa motifs (Selvi et al., 2010). We

(D) Identification of GSE-interacting protein with a cDNA library of the mouse ovary using a yeast two-hybrid assay. Letters A to F indicate the positions in the dish.
(E) Identification of a Mettl23-binding region of GSE using a yeast two-hybrid assay. The region derived from exons 4 and 5 was responsible for binding with Mettl23.
(F) Interaction of GSE with Mettl23 in PN3 zygotes, as demonstrated by coimmunoprecipitation using specific antibodies. A representative result from three replicate experiments each using 100–150 zygotes.
(G) Direct interaction of GSE and Mettl23 confirmed by immunoprecipitation followed by immunoblotting using His-GSE and His-Mettl23 purified from transfected HEK293 cells. A representative result from three replicate experiments. sup, supernatant.

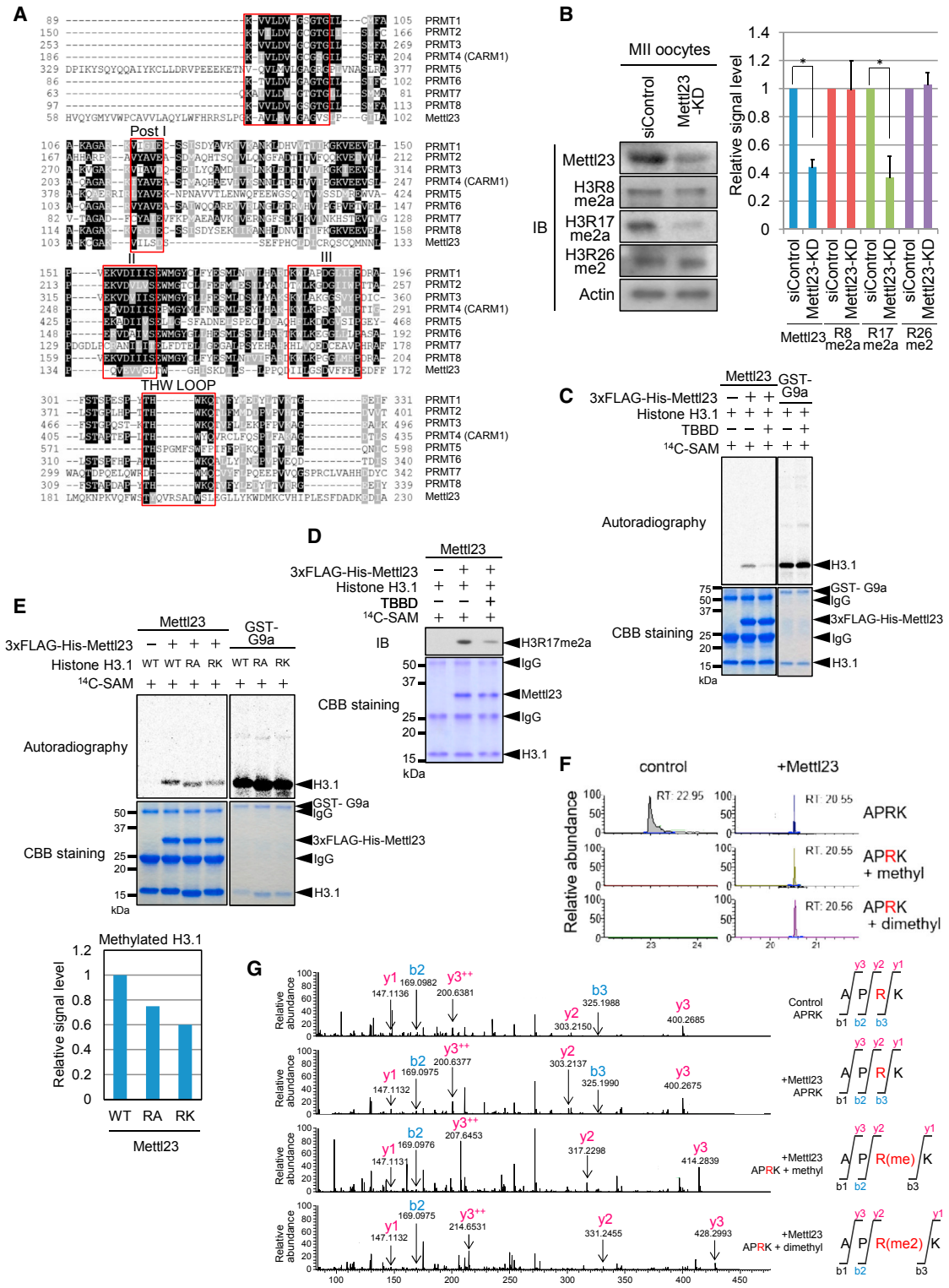

Figure 2. Arginine Methylation Activity of Mettl23 Protein

(A) Amino acid sequence alignment of the methyltransferase I region of mouse Mettl23, together with PRMT1–8. The same amino acids are shaded in black, and similar amino acids are shaded in gray. Conserved signature methyltransferase motifs are boxed in red.

(B) The effect of Mettl23-KD on the methylation of different arginine residues of histone H3 in oocytes. The graph on the right indicates relative band intensities. The level of actin was set as 1.0. Results from three replicate experiments (about 30 oocytes each). *$p < 0.001$ (versus siControl). Error bars indicate SEM.

(legend continued on next page)

also found a reduction in the level of H3R17me2a in the presence of TBBD using anti-H3R17me2a antibody by immunoblot analysis (Figure 2D). We identified the localization of CARM1 (also known as PRMT4), another H3R17me2a PRMT. It was localized in the cytoplasm, but not in the PNs, of zygotes (Figure S2C) and in the nucleus and cytoplasm of GV oocytes (Figure S2E). Then, to clarify whether the methylation activity of Mettl23 was CARM1 dependent, we performed co-immunoprecipitation experiments using anti-FLAG and anti-CARM1 antibodies in the mixture of purified 3xFLAG-His6-Mettl23. We found that Mettl23 did not interact with CARM1 (Figure S2F), indicating that the H3.1R17me2a was methylated by Mettl23 but not by CARM1.

To confirm that H3R17 was the target of Mettl23, we investigated the effect of unmethylatable R17 mutants, H3.1R17A and H3.1R17K, on the Mettl23 activity in vitro. These mutations resulted in the reduction of the levels of H3.1 methylation, as indicated by the alterations in signal intensity (H3.1R17A, 0.75; and H3.1R17K, 0.60 [WT = 1.0]) (Figure 2E). This result indicated that Mettl23 methylated H3R17, although it might also methylate other residues of H3 in vitro. In MII oocytes, however, Mettl23 did not methylate H3R8 or H3R26, at least at the immunoblot level (Figure 2B).

To identify the accumulation of R17 methylation by Mettl23, we next analyzed the resulting $H3.1_{15–18}$ peptide containing R17, APRK peptide, by mass spectrometry. The mono- and dimethylated APRK peptides could be detected in the presence of 3xFLAG-His6-Mettl23 with recombinant H3.1 (Figure 2F). We also found a tandem mass spectroscopy spectrum of mono- and dimethylation on R17 (Figure 2G). These results collectively suggest that Mettl23 catalyzes dimethylation of H3R17.

GSE and Mettl23 Are Indispensable for 5mC Oxidation by Recruiting Tet3

To determine the function of GSE and Mettl23 in 5mC oxidation during zygote development, we generated GSE gene knockout (GSE-KO) and Mettl23 gene knockout (Mettl23-KO) mice by the CRISPR/Cas9 system (Figure S3A). Mice carrying homozygous mutations were born alive in both KO lines. We confirmed the successful deletions of GSE and Mettl23 in the KO mice by western blot analysis using their testes (Figure S3B). Homozygous mutant mice from the GSE-KO line were indistinguishable from their heterozygous counterparts in terms of gross appearance, growth rate (data not shown), and reproductive performance, such as litter sizes (Figure S3C). By contrast, the Mettl23-KO line gave birth to significantly smaller litter sizes following homozygous mating, compared with heterozygous mating (Figure S3C). Moreover, about 33% (11/33) of the homozygous Mettl23 newborn mice died before weaning from unknown causes, and only a few survived to adulthood. Because Mettl23 is ubiquitously expressed in many tissues (Figure S1C), and the PRMTs and Mettl families might catalyze nonhistone proteins (Blanc and Richard, 2017; Shimazu et al., 2014), these Mettl23-KO phenotypes might be attributable to the loss of systemic, multifunctional catalytic activity of this enzyme.

In zygotes derived from GSE-KO or Mettl23-KO oocytes, the 5mC level remained high and the 5hmC level remained low in the male PN (Figures 3A, S4A, and S4B). The injection of Mettl23 mRNA into Mettl23-KO oocytes restored the conversion of 5mC to 5hmC in maternal Mettl23-KO zygotes (Figures 3A, S4A, and S4B). These findings indicated that GSE-KO or Mettl23-KO in oocytes resulted in the failure of the 5mC-to-5hmC conversion. This impaired 5mC oxidation was confirmed by methylated DNA immunoprecipitation (MeDIP) and hydroxymethylated DNA immunoprecipitation (hMeDIP) experiments directed to the *Line1* retrotransposon regions, which are known to be actively demethylated in zygotes (Gu et al., 2011; Wossidlo et al., 2010). The 5mC level at *Line1* was higher in maternal GSE-KO or Mettl23-KD zygotes than in siRNA-treated control (siControl) zygotes, while the 5hmC level was lower in these knockdown zygotes (Figure 3B). Furthermore, our chromatin immunoprecipitation (ChIP) analysis using about 1,400 intact zygotes revealed that H3R17me2a was enriched at the *Line1* regions (Figure 3C). All these findings suggest that maternal GSE and Mettl23, in association with H3R17me2a, can play essential roles in the oxidation of 5mC to 5hmC in zygotes, although this is not a required event for viability.

We next observed Tet3 localization in maternal GSE-KO and Mettl23-KO zygotes. In control zygotes, Tet3 was localized in both male and female PNs, with a stronger intensity in the male PN (Figure 3D), as reported previously (Guo et al., 2014; Shen et al., 2014). The Tet3 signal was significantly reduced in GSE- or Mettl23-KO zygotes compared with the wild-type (WT) (Figures 3D and S4C). The forced expression of Mettl23 in its KO zygotes restored the accumulation of Tet3 into the male PN (Figures 3D and S4C). These results indicated that Mettl23

(C) Mettl23 methylates histone H3.1 in vitro. 3xFLAG-His6-Mettl23 was tandem affinity purified from transfected HEK293T cells. GST-fused catalytic domain of G9a, which is known as H3K9 methyltransferase, was used as positive control for the methylation assay. The H3R17 methylation inhibitor TBBD (final, 100 μM) impaired methylation by Mettl23, but not by G9a. Top: autoradiography. Bottom: Coomassie brilliant blue (CBB) stain. CBB staining was performed as an equal loading control.

(D) Asymmetric dimethylation at arginine 17 of histone H3 (H3R17me2a) induced by Mettl23 in vitro. The H3R17 methylation inhibitor TBBD (final, 100 μM) impaired the methylation by Mettl23.

(E) Effect of unmethylatable mutations of H3.1R17 on the accumulation of H3.1 methylation in the presence of 14C-SAM in vitro. Top: autoradiography indicating the methylation signals of H3.1 induced by Mettl23. CBB staining was performed as an equal loading control. The mutations of H3.1R17 did not change the methylation levels induced by the GST-fused catalytic domain of G9a. Bottom: the relative methylated H3.1 signal intensities in the mutations by Mettl23. The level of CBB stain was set as 1.0.

(F) Selected ion chromatograms of y3 ions (m/z = 400.267, 414.283, and 428.299; see Figure 2G) that from the parent ions of unmethylated (me0), monomethylated (me1) and dimethylated (me2) forms of APRK peptides obtained from digestion of recombinant H3.1 with or without Mettl23. Predicted methylation sites are indicated in red. RT indicates retention time of the displayed ion chromatograms. m/z, mass-to-charge ratio.

(G) Tandem mass spectrometry (MS/MS) spectra of the three methylation states of APRK peptides with Mettl23. The indicated b (blue) and y (pink) ions indicate mono- and dimethylation on the arginine.

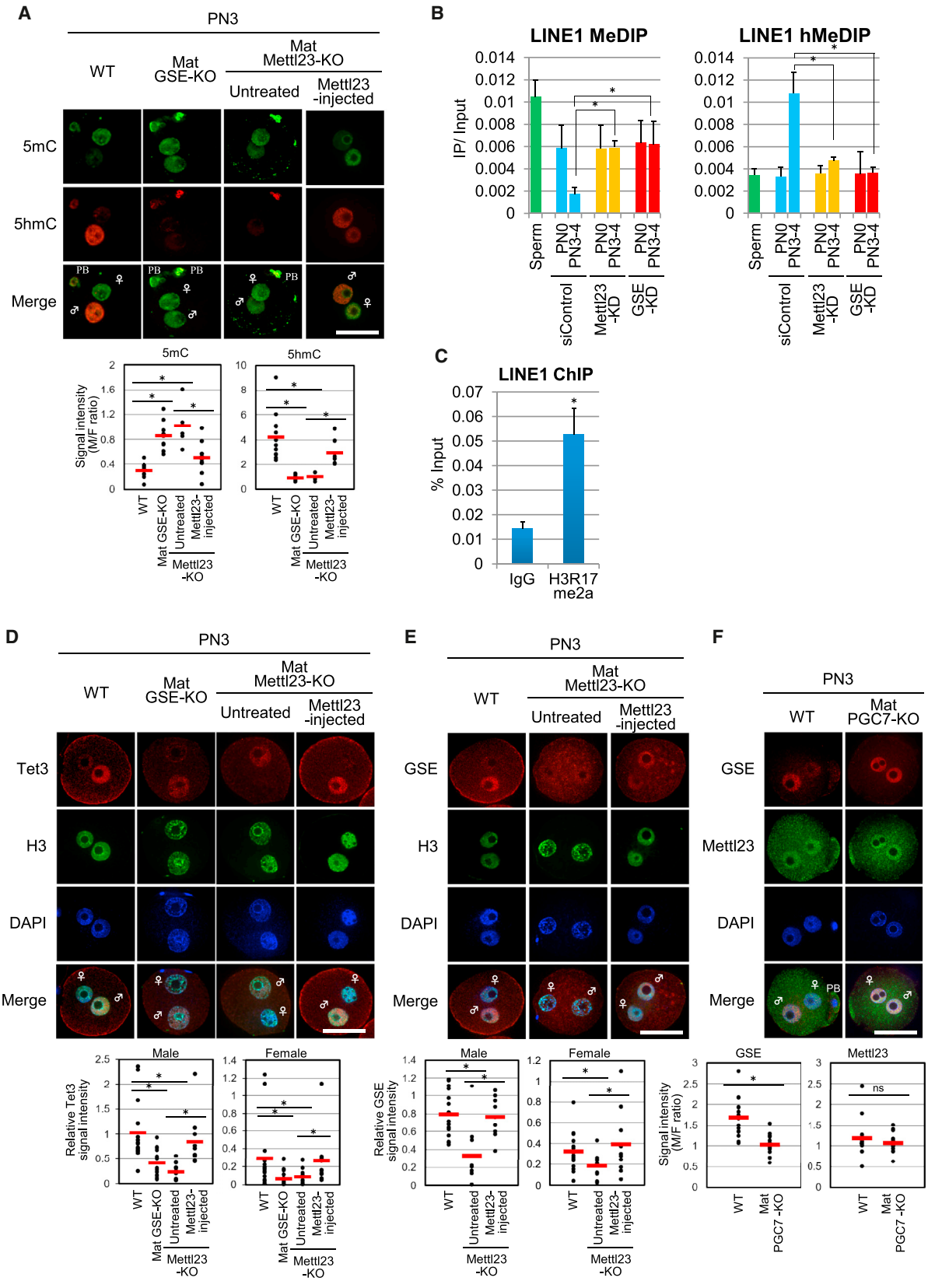

(legend on next page)

and GSE are involved in Tet3 localization in the PNs. Next, we examined whether Mettl23-KO might affect localization of the GSE protein in the PNs, because it was possible that Mettl23 might function as a recruiter of GSE-Tet3 to the target sites. As expected, only faint signals for GSE were found in the PNs of the Mettl23-KO zygotes, and the rescue experiment resulted in recruitment of GSE into the male PN (Figure 3E). Taken together with the results from the biochemical analyses discussed earlier, it is likely that maternal Mettl23 is responsible for 5mC oxidation by recruiting the GSE-Tet3 complex into the chromatin during zygote development. It also suggests that CARM1 is not able to compensate for the function of Mettl23 in active DNA demethylation.

PGC7 Is Responsible for the Asymmetric Localization of GSE-Tet3 in PNs

It is known that the asymmetrical pattern of active DNA demethylation between the paternal and maternal genomes is achieved by the presence of the PGC7 protein, which protects the female genome from Tet3 (Nakamura et al., 2007). Therefore, we examined whether the localization patterns of GSE and Mettl23 in zygotes might be altered by deletion of the maternal PGC7. In maternal PGC7 KO zygotes, the fluorescence intensity for GSE in the female PN increased approximately to the level of that in the male PN, the male/female (M/F) fluorescence ratio becoming ~1 (Figure 3F). By contrast, the fluorescence levels of Mettl23 were unchanged and very similar between the male and female PNs in the same zygotes (Figure 3F). These findings indicate that PGC7 protects the maternal genome from GSE-Tet3, while the attachment of Mettl23 to both parental genomes is not influenced by the presence of PGC7.

Methylation at R17 Is Essential for H3.3 Incorporation into the Male PN

As both CARM1 and Mettl23 are present in the cytoplasm of unfertilized oocytes, it is possible that maternal histone H3.3 has been modified with R17me2a before fertilization. To assess this possibility, we injected oocytes with mRNA for EGFP -tagged H3.3 with amino acid substitutions. Normal H3.3, as well as R8- and R26-mutated H3.3, was incorporated into the male PN, whereas R17-mutated H3.3 failed to be localized into the male PN (Figure 4). This result indicated that methylation at R17 may be a prerequisite for H3.3 incorporation into the paternal nucleosomes.

DISCUSSION

Reprogramming of the paternal genome at fertilization is one of the most dynamic epigenetic changes during the life cycle in mammals. Here, we identified H3R17me2a as a histone modification that may regulate the reprogramming of the paternal genome through protamine-histone exchange and active DNA demethylation. A large part—if not all—of the R17me2a modification on H3.3 in the oocytes/zygotes may be attributable to the activity of Mettl23, here reported to have PRMT. A key question that remains unanswered is why H3R17me2a is the essential histone modification for reprogramming of the paternal genome. It is known that H3R17me2a is frequently associated with transcriptionally active chromatin (Chen et al., 1999; Di Lorenzo and Bedford, 2011; Wu et al., 2009). In addition, conversion of 5mC to 5hmC occurs on transcriptionally active euchromatin in mouse embryonic stem cells and human somatic cells (Ficz et al., 2011; Kubiura et al., 2012). Therefore, we postulate that Mettl23-catalyzed H3R17me2a might induce an open chromatin structure so that the subsequent molecular events can proceed normally until the full reprogramming of the paternal genome. Generally, information on reader proteins that recognize methylated arginine is limited, compared with that on lysine methylation (Musselman et al., 2012). A recent study suggested that the TDRD3 Tudor domain, which recognizes H3R17me2a and H4R3me2a, was tightly complexed with DNA topoisomerase IIIβ (TOP3B) to induce relaxation of negative supercoiled DNA in cultured cells (Yang et al., 2014). It would be interesting to see whether a similar mechanism is active at the H3R17me2a sites in zygotes.

When sperm enters an egg, it must undergo biochemical remodeling that is reliant on maternal factors. Decondensation of the sperm head takes place by maternal nucleoplasmin 2, releasing protamine into the oocyte cytoplasm, in preparation for PN formation. It is known that de novo nucleosome assembly is dependent on H3.3 and its chaperone Hira, which is essential for PN formation (Inoue and Zhang, 2014; Nashun et al., 2015). In this study, we found that H3.3 devoid of R17me2a was unable to participate in PN formation, suggesting that the R17me2a modification was a prerequisite for nucleosome assembly by

Figure 3. GSE and Mettl23 Are Indispensable for Active DNA Demethylation by Recruiting Tet3 to the PNs

(A) Top: representative immunofluorescence images of 5mC and 5hmC in different groups of PN3 zygotes. PB, the second polar body. Scale bar, 50 μm. Bottom: the fluorescence M/F ratios for 5mC and 5hmC. Each dot represents a single zygote (11 zygotes for each group). Red bars indicate the mean ratios. *$p < 0.001$ (versus WT).

(B) qPCR analysis of *Line1* regions on immunoprecipitation using an anti-5mC antibody (for MeDIP) and anti-5hmC antibody (for hMeDIP). Results are from 30 oocytes (PN0) or 30 PN3–4 zygotes. *$p < 0.05$. Error bars indicate SEM. Results from three biological replicate experiments. The values for PN0 were calculated by adding the values of spermatozoa to those of MII oocytes.

(C) ChIP analysis of H3R17me2a on *Line1* regions. Results are from three biological replicate experiments. *$p < 0.05$. Error bars indicate SEM.

(D) Top: representative immunofluorescence images of Tet3 in maternal GSE-KO or Mettl23-KO zygotes. H3 is indicated in green as a control for chromatin-bound factors. DNA was stained with DAPI. PB, the second polar body. Scale bar, 50 μm. Bottom: the relative Tet3 signal intensities in the male and female PNs. The numbers of zygotes analyzed were 10 to 15 for each group. The level of H3 was set as 1.0. Red bars indicate the mean ratios. *$p < 0.001$ (versus WT).

(E) Top: representative immunofluorescence images of GSE in Mettl23-KO zygotes. Bottom: the relative GSE signal intensities in the male and female PNs. For other information see the legend for Figure 3D.

(F) Immunofluorescence images of GSE and Mettl23 in maternal PGC7-KO zygotes. The M/F ratio for the GSE level was significantly reduced (*$p < 0.005$), but the Mettl23 level was unchanged. Fifteen zygotes were analyzed for each group. For other information, see the legend for (D). ns, not significant.

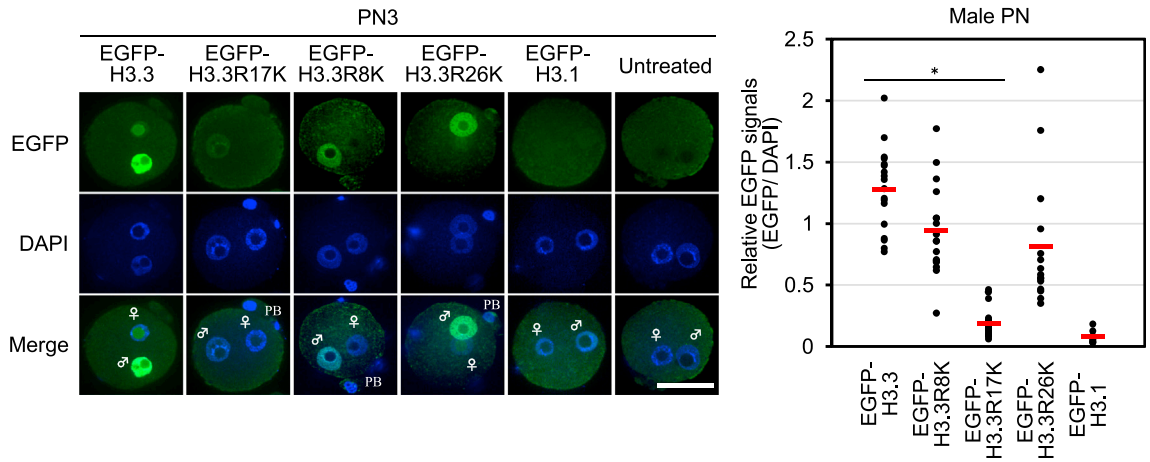

Figure 4. H3R17me2a Is Essential for Maternal H3.3 Incorporation into the Male PN

Effect of an unmethylatable mutation of H3.3R17 on deposition into paternal nucleus by injection of EGFP-fused histone mutants. Left: immunofluorescence images of EGFP in mRNA-injected zygotes. Right: the EGFP signal intensity in male PN. Each dot represents a single zygote. The numbers of zygotes analyzed were 11 to 20 for each group. Red bars indicate the mean ratios. Asterisks indicate significant differences compared with control embryos ($p < 0.05$). PB, the second polar body. Scale bar, 50 μm.

H3.3. Our experimental results indicate that the enzymatic activity of Mettl23 as R17me2a PRMT is exerted before fertilization (Figure 2B). This may result in accumulation of H3.3R17me2a in the MII ooplasm, which may induce paternal nucleosomal assembly upon fertilization. Because Mettl23 knockout oocytes normally form PNs, it is probable that the catalytic role of Mettl23 might be compensated for—at least in part—by CARM1, another R17me2a PRMT, during paternal nucleosome formation. The abundant localization of CARM1 in the immature oocytes may support this assumption (Torres-Padilla et al., 2007). Generation of oocytes lacking both Mettl23 and CARM1 would help solve these questions. Mettl23 has distant homology with other PRMTs (Figure 2A), and two point mutations of the putative catalytic sites (D113V and D163V) still retained the enzymatic activity (unpublished data). This may suggest that the active site or reaction mechanism of Mettl23 is different from that of other PRMTs. If another unidentified H3R17 PRMT exists in oocytes, Mettl23 might interact with it as a partner protein.

In contrast to the obvious involvement of Mettl23 in H3R17me2a formation before PN formation, its involvement in active DNA demethylation remains to be studied. After PN formation, Mettl23, but not CARM1, was localized in the PNs and bound to GSE, a Tet3-interacting protein. Therefore, Mettl23 may have some non-PRMT role in Tet3-mediated active DNA demethylation, which CARM1 does not possess. Depletion of Mettl23 resulted in impaired pronuclear localization of GSE, Tet3, and 5hmC, indicating that Mettl23 functions as a recruiter of GSE and Tet3 to target sites. A structural analysis of Mettl23 could elucidate the mechanisms underlying its multifunction. Indeed, Mettl23 has low homology to all the PRMTs in their non-conserved domains (Figure 2A). CARM1 is known to be a multifunctional protein and is engaged in non-PRMT roles, such as mRNA processing (Cheng et al., 2007) and regulating protein stability (Feng et al., 2006). Thus, Mettl23 and CARM1 have the PRMT activity in oocytes and zygotes by the common conserved domains, while Mettl23 might have another function as a recruiter of GSE-Tet3.

One of the important features of active DNA demethylation in zygotes is its predominant contribution to reprogramming of the paternal genome (Mayer et al., 2000), although this event is not essential for subsequent embryonic development (Inoue et al., 2015). This parental-origin-dependent DNA demethylation is ensured by the preferential localization of maternal PGC7 to the female PN (Nakamura et al., 2007). The female PN is enriched with H3K9me2, which attracts the PGC7 protein to the maternal genome. It was shown experimentally that PGC7 protected 5mC from Tet3-mediated oxidation (Nakamura et al., 2012). Detailed biochemical analyses using isolated male and female PNs revealed that conversion of 5mC to 5hmC by Tet3 also occurs in the female PN, albeit on a smaller scale (Guo et al., 2014; Shen et al., 2014). These studies also identified target regions of active DNA demethylation, some of which were specific for either the maternal or the paternal genome. Our study provides another layer of information to explain this process. We found that GSE was preferentially localized to the male PN, while Mettl23-H3R17me2a was evenly distributed in both PNs. Interestingly, maternal PGC7-KO resulted in elevation of the GSE level as well as the Tet3 level in the female PN. This finding supports the idea that while Mettl23-H3R17me2a can be localized to the maternal (oocyte) genome, H3K9me2-PGC7 inhibits the attachment of GSE-Tet3 to Mettl23, thus preventing active DNA demethylation in the female PN. Thus, active DNA demethylation in zygotes may be regulated by two different histone modifications, H3R17me2a and H3K9me2, which have opposite effects on Tet3 recruitment.

EXPERIMENTAL PROCEDURES

Detailed methods are available in the Supplemental Information.

Animals

All animal experiments described here were approved by the Animal Experimentation Committees at the RIKEN Tsukuba Institute and Kinki University and were performed in accordance with the committees' guiding principles. Animals were housed under controlled lighting conditions (daily light, 0700–2100 hr) and were maintained under specific pathogen-free conditions.

Immunocytochemistry and Microscopy

The classification of PN stages was performed according to previous studies (Santos et al., 2002; Wossidlo et al., 2010), where the pronuclear morphology and hours postinsemination were taken into consideration. Oocytes or zygotes were treated with 0.2% Triton X-100 (Nacalai Tesque) in PBS for 30 s, washed with PBS three times, and fixed in 4% PFA (Nacalai Tesque) (Nakamura et al., 2012). In some experiments (Figure 4A), oocytes or embryos were fixed in 4% PFA first, followed by treatment with PBS containing 0.1%–0.2% Triton X-100 at room temperature (RT) for 1 hr. For 5mC, 5hmC, and DNA, the specimens were incubated in 4 N HCl at RT for 30 min and then incubated in 0.1 M EDTA at RT for 30 min. They were then incubated with the primary antibodies (Table S1) in PBS containing 30 mg/mL BSA at 4°C overnight. After washing, they were reacted with the secondary antibodies as appropriate (Table S1) at RT for 1 hr. Specimens were mounted on glass slides in Vectashield mounting medium (Vector Laboratories) containing 2–5 μg/mL DAPI (Invitrogen; D1306). Finally, the slides were imaged using a CellVoyager CV1000 confocal scanner system (Yokogawa Electric). ImageJ software (NIH, Bethesda, MD, USA; http://rsbweb.nih.gov/ij/) was used to quantify DAPI staining and antibody signals in the central region of each PN. At least three independent replicates were performed for each experiment.

ChIP

These procedures were performed essentially as described (Hatanaka et al., 2015). In brief, about 1,400 mouse zygotes were harvested for cross-linking. Fixation and isolation of the nuclei of the zygotes were performed using truChIP Chromatin Shearing Reagent Kits (Covaris). Chromatin shearing was performed using a Covaris S220 instrument. Immunoprecipitation was performed as described earlier. For binding to magnetic beads, each antibody was incubated with Dynabeads Protein G (Invitrogen) in a ChIP dilution buffer containing 0.01% SDS, 1.1% w/v Triton X-100, 1.2 mM EDTA, and 167 mM NaCl at 4°C for 1 hr with rotation. After washing, the beads were incubated with the chromatin shearing solution at 4°C for 6 hr with rotation. After immunoprecipitation, the beads were washed using a low-salt wash buffer containing 20 mM Tris-HCl, 0.1% SDS, 1% w/v Triton X-100, 2 mM EDTA, and 150 mM NaCl and a high-salt wash buffer containing 20 mM Tris-HCl, 0.1% SDS, 1% w/v Triton X-100, 2 mM EDTA, and 500 mM NaCl. For elution of the DNA from the beads, they were incubated with ChIP direct elution buffer containing 10 mM Tris-HCl, 1% SDS, 5 mM EDTA, and 300 mM NaCl at 4°C for 15 min with rotation. The solution was incubated at 65°C overnight and then treated with proteinase K and RNase A and subjected to DNA purification. Prepared DNA samples were amplified and analyzed by qRT-PCR. The primers used are described in Table S2. Amplifications were run in a 7900HT Sequence Detector System (Applied Biosystems).

Statistical Analysis

For statistical analysis, we performed one-way ANOVA using StatView v.5.0 (SAS Institute) or Microsoft Excel. A post hoc procedure using Fisher Protected Least Significant Difference (PLSD) was adopted for multiple comparisons between the groups where appropriate. The p values < 0.05 were considered significant.

SUPPLEMENTAL INFORMATION

Supplemental Information includes Supplemental Experimental Procedures, four figures, and two tables and can be found with this article online at http://dx.doi.org/10.1016/j.celrep.2017.08.088.

AUTHOR CONTRIBUTIONS

Y. Hatanaka, K. Matsumoto, and A.O. conceived the project and designed the research. Y. Hatanaka, T.T., N.S., K. Morita, T.S., S.M., M.S., A.H., M.H., S.K., N.O., and K.I. performed the experiments. Y. Hatanaka, T. Nakamura, Y. Hosoi, N.D., T. Nakano, H.K., K. Matsumoto, Y.S., and A.O. analyzed the data and discussed the research. Y. Hatanaka and A.O. wrote the paper.

ACKNOWLEDGMENTS

The authors wish to thank Dr. Guoliang Xu for the anti-Tet3 antibody and Dr. Tadahiro Shimazu for the suggestion of an in vitro assay of Mettl23 activity. This study was supported by JSPS KAKENHI grant numbers JP25112009 (to A.O.), JP23220011 (to A.O.), JP25292189 (K.M.), JP25116002 (to H.K.), and JP15K18545 (to Y. Hatanaka) and by the RIKEN Epigenetics Program (Strategic Programs for R&D) (to A.O. and Y.S.), the RIKEN Incentive Research Projects 2015 (to Y. Hatanaka) and 2016 (to Y. Hatanaka), and the RIKEN Junior Research Associate Program (to T.T.).

Received: November 22, 2016
Revised: May 31, 2017
Accepted: August 25, 2017
Published: September 19, 2017

REFERENCES

Blanc, R.S., and Richard, S. (2017). Arginine methylation: The coming of age. Mol. Cell *65*, 8–24.

Chen, D., Ma, H., Hong, H., Koh, S.S., Huang, S.M., Schurter, B.T., Aswad, D.W., and Stallcup, M.R. (1999). Regulation of transcription by a protein methyltransferase. Science *284*, 2174–2177.

Cheng, D., Côté, J., Shaaban, S., and Bedford, M.T. (2007). The arginine methyltransferase CARM1 regulates the coupling of transcription and mRNA processing. Mol. Cell *25*, 71–83.

Cloutier, P., Lavallée-Adam, M., Faubert, D., Blanchette, M., and Coulombe, B. (2013). A newly uncovered group of distantly related lysine methyltransferases preferentially interact with molecular chaperones to regulate their activity. PLoS Genet. *9*, e1003210.

Di Lorenzo, A., and Bedford, M.T. (2011). Histone arginine methylation. FEBS Lett. *585*, 2024–2031.

Feng, Q., Yi, P., Wong, J., and O'Malley, B.W. (2006). Signaling within a coactivator complex: methylation of SRC-3/AIB1 is a molecular switch for complex disassembly. Mol. Cell. Biol. *26*, 7846–7857.

Ficz, G., Branco, M.R., Seisenberger, S., Santos, F., Krueger, F., Hore, T.A., Marques, C.J., Andrews, S., and Reik, W. (2011). Dynamic regulation of 5-hydroxymethylcytosine in mouse ES cells and during differentiation. Nature *473*, 398–402.

Gu, T.P., Guo, F., Yang, H., Wu, H.P., Xu, G.F., Liu, W., Xie, Z.G., Shi, L., He, X., Jin, S.G., et al. (2011). The role of Tet3 DNA dioxygenase in epigenetic reprogramming by oocytes. Nature *477*, 606–610.

Guo, F., Li, X., Liang, D., Li, T., Zhu, P., Guo, H., Wu, X., Wen, L., Gu, T.P., Hu, B., et al. (2014). Active and passive demethylation of male and female pronuclear DNA in the mammalian zygote. Cell Stem Cell *15*, 447–458.

Hackett, J.A., Zylicz, J.J., and Surani, M.A. (2012). Parallel mechanisms of epigenetic reprogramming in the germline. Trends Genet. *28*, 164–174.

Hatanaka, Y., Shimizu, N., Nishikawa, S., Tokoro, M., Shin, S.W., Nishihara, T., Amano, T., Anzai, M., Kato, H., Mitani, T., et al. (2013). GSE is a maternal factor involved in active DNA demethylation in zygotes. PLoS ONE *8*, e60205.

Hatanaka, Y., Inoue, K., Oikawa, M., Kamimura, S., Ogonuki, N., Kodama, E.N., Ohkawa, Y., Tsukada, Y., and Ogura, A. (2015). Histone chaperone CAF-1 mediates repressive histone modifications to protect preimplantation mouse embryos from endogenous retrotransposons. Proc. Natl. Acad. Sci. USA *112*, 14641–14646.

Inoue, A., and Zhang, Y. (2011). Replication-dependent loss of 5-hydroxymethylcytosine in mouse preimplantation embryos. Science *334*, 194.

Inoue, A., and Zhang, Y. (2014). Nucleosome assembly is required for nuclear pore complex assembly in mouse zygotes. Nat. Struct. Mol. Biol. *21*, 609–616.

Inoue, A., Shen, L., Matoba, S., and Zhang, Y. (2015). Haploinsufficiency, but not defective paternal 5mC oxidation, accounts for the developmental defects of maternal Tet3 knockouts. Cell Rep. *10*, 463–470.

Kohli, R.M., and Zhang, Y. (2013). TET enzymes, TDG and the dynamics of DNA demethylation. Nature *502*, 472–479.

Kubiura, M., Okano, M., Kimura, H., Kawamura, F., and Tada, M. (2012). Chromosome-wide regulation of euchromatin-specific 5mC to 5hmC conversion in mouse ES cells and female human somatic cells. Chromosome Res. *20*, 837–848.

Lin, C.J., Koh, F.M., Wong, P., Conti, M., and Ramalho-Santos, M. (2014). Hira-mediated H3.3 incorporation is required for DNA replication and ribosomal RNA transcription in the mouse zygote. Dev. Cell *30*, 268–279.

Mayer, W., Niveleau, A., Walter, J., Fundele, R., and Haaf, T. (2000). Demethylation of the zygotic paternal genome. Nature *403*, 501–502.

Mizuno, S., Sono, Y., Matsuoka, T., Matsumoto, K., Saeki, K., Hosoi, Y., Fukuda, A., Morimoto, Y., and Iritani, A. (2006). Expression and subcellular localization of GSE protein in germ cells and preimplantation embryos. J. Reprod. Dev. *52*, 429–438.

Musselman, C.A., Lalonde, M.E., Côté, J., and Kutateladze, T.G. (2012). Perceiving the epigenetic landscape through histone readers. Nat. Struct. Mol. Biol. *19*, 1218–1227.

Nakamura, T., Arai, Y., Umehara, H., Masuhara, M., Kimura, T., Taniguchi, H., Sekimoto, T., Ikawa, M., Yoneda, Y., Okabe, M., et al. (2007). PGC7/Stella protects against DNA demethylation in early embryogenesis. Nat. Cell Biol. *9*, 64–71.

Nakamura, T., Liu, Y.J., Nakashima, H., Umehara, H., Inoue, K., Matoba, S., Tachibana, M., Ogura, A., Shinkai, Y., and Nakano, T. (2012). PGC7 binds histone H3K9me2 to protect against conversion of 5mC to 5hmC in early embryos. Nature *486*, 415–419.

Nashun, B., Yukawa, M., Liu, H., Akiyama, T., and Aoki, F. (2010). Changes in the nuclear deposition of histone H2A variants during pre-implantation development in mice. Development *137*, 3785–3794.

Nashun, B., Hill, P.W., Smallwood, S.A., Dharmalingam, G., Amouroux, R., Clark, S.J., Sharma, V., Ndjetehe, E., Pelczar, P., Festenstein, R.J., et al. (2015). Continuous histone replacement by Hira is essential for normal transcriptional regulation and de novo DNA methylation during mouse oogenesis. Mol. Cell *60*, 611–625.

Pastor, W.A., Aravind, L., and Rao, A. (2013). TETonic shift: biological roles of TET proteins in DNA demethylation and transcription. Nat. Rev. Mol. Cell Biol. *14*, 341–356.

Santos, F., Hendrich, B., Reik, W., and Dean, W. (2002). Dynamic reprogramming of DNA methylation in the early mouse embryo. Dev. Biol. *241*, 172–182.

Sasaki, H., and Matsui, Y. (2008). Epigenetic events in mammalian germ-cell development: reprogramming and beyond. Nat. Rev. Genet. *9*, 129–140.

Selvi, B.R., Batta, K., Kishore, A.H., Mantelingu, K., Varier, R.A., Balasubramanyam, K., Pradhan, S.K., Dasgupta, D., Sriram, S., Agrawal, S., and Kundu, T.K. (2010). Identification of a novel inhibitor of coactivator-associated arginine methyltransferase 1 (CARM1)-mediated methylation of histone H3 Arg-17. J. Biol. Chem. *285*, 7143–7152.

Shen, L., Inoue, A., He, J., Liu, Y., Lu, F., and Zhang, Y. (2014). Tet3 and DNA replication mediate demethylation of both the maternal and paternal genomes in mouse zygotes. Cell Stem Cell *15*, 459–470.

Shimazu, T., Barjau, J., Sohtome, Y., Sodeoka, M., and Shinkai, Y. (2014). Selenium-based S-adenosylmethionine analog reveals the mammalian seven-beta-strand methyltransferase METTL10 to be an EF1A1 lysine methyltransferase. PLoS ONE *9*, e105394.

Tan, L., and Shi, Y.G. (2012). Tet family proteins and 5-hydroxymethylcytosine in development and disease. Development *139*, 1895–1902.

Torres-Padilla, M.E., Parfitt, D.E., Kouzarides, T., and Zernicka-Goetz, M. (2007). Histone arginine methylation regulates pluripotency in the early mouse embryo. Nature *445*, 214–218.

Wossidlo, M., Arand, J., Sebastiano, V., Lepikhov, K., Boiani, M., Reinhardt, R., Schöler, H., and Walter, J. (2010). Dynamic link of DNA demethylation, DNA strand breaks and repair in mouse zygotes. EMBO J. *29*, 1877–1888.

Wu, Q., Bruce, A.W., Jedrusik, A., Ellis, P.D., Andrews, R.M., Langford, C.F., Glover, D.M., and Zernicka-Goetz, M. (2009). CARM1 is required in embryonic stem cells to maintain pluripotency and resist differentiation. Stem Cells *27*, 2637–2645.

Yang, Y., McBride, K.M., Hensley, S., Lu, Y., Chedin, F., and Bedford, M.T. (2014). Arginine methylation facilitates the recruitment of TOP3B to chromatin to prevent R loop accumulation. Mol. Cell *53*, 484–497.